Physics Letters B 775 (2017) 25–31

Contents lists available at ScienceDirect

Physics Letters B

www.elsevier.com/locate/physletb

Single top quark production as a probe of anomalous $tq\gamma$ and tqZ couplings at the FCC-ee

Hamzeh Khanpour [a,b], Sara Khatibi [b], Morteza Khatiri Yanehsari [c], Mojtaba Mohammadi Najafabadi [b]

[a] Department of Physics, University of Science and Technology of Mazandaran, P.O. Box 48518-78195, Behshahr, Iran
[b] School of Particles and Accelerators, Institute for Research in Fundamental Sciences (IPM), P.O. Box 19395-5531, Tehran, Iran
[c] School of Physics, Institute for Research in Fundamental Sciences (IPM), P.O. Box 19395-5531, Tehran, Iran

ARTICLE INFO

Article history:
Received 30 March 2017
Received in revised form 20 October 2017
Accepted 22 October 2017
Available online xxxx
Editor: G.F. Giudice

ABSTRACT

In this paper, a detailed study to probe the top quark Flavour-Changing Neutral Currents (FCNC) $tq\gamma$ and tqZ at the future e^-e^+ collider FCC-ee in two different center-of-mass energies of 240 and 350 GeV is presented. A set of useful variables are proposed and used in a multivariate technique to separate signal $e^-e^+ \to Z/\gamma \to t\bar{q}$ $(\bar{t}q)$ from Standard Model background processes. The study includes a fast detector simulation based on the DELPHES package to consider the detector effects. The upper limits on the FCNC branching ratios at 95% confidence level (CL) in terms of the integrated luminosity are presented. It is shown that with 300 fb^{-1} of integrated luminosity of data, FCC-ee would be able to exclude the effective coupling strengths above $\mathcal{O}(10^{-4} - 10^{-5})$ which is corresponding to branching fraction of $\mathcal{O}(0.01 - 0.001)$%. We show that moving to a high-luminosity regime leads to a significant improvement on the upper bounds on the top quark FCNC couplings to a photon or a Z boson.

1. Introduction

The top quark with its large mass and very short life time is one of the most interesting discovered particles in the Standard Model (SM). Studying the top quark enables us to investigate the electroweak symmetry breaking mechanism (EWSB) as well as searching for extensions of the SM. In the framework of the SM, top-quark Flavour-Changing Neutral Currents (FCNC) only arise at loop level and are highly suppressed because of the GIM (Glashow–Iliopoulos–Maiani) mechanism [1]. For instance, the SM predictions for the branching fractions of FCNC processes like $t \to \gamma u(c)$ and $t \to Zu(c)$ are of the order of $10^{-16}(10^{-14})$ and $10^{-17}(10^{-14})$, respectively [2]. The ability of the present experiments is far from measuring such tiny branching ratios. On the other hand, several extensions of the SM such as Technicolor, SUSY models, two Higgs doublet models predict much higher branching ratios up to $10^8 - 10^9$ order of magnitude larger than SM predictions [2–10]. Consequently, any observation of these rare FCNC transitions would be a clear signal of new physics beyond the SM.

So far, there are several experimental studies searching for FCNC transitions of the top quark to a photon or a Z boson through different channels [11–26]. The most stringent observed upper limits at 95% confidence level (CL) have been found to be [11,13,27]:

$$\begin{aligned} \text{CMS:}\quad & Br(t \to Zu) < 0.017\%, \\ & Br(t \to Zc) < 0.020\%, \\ \text{ATLAS:}\quad & Br(t \to Zq) < 0.07\% \text{ (observed)}, \\ \text{CMS:}\quad & Br(t \to u\gamma) < 0.013\%, \\ & Br(t \to c\gamma) < 0.170\%. \end{aligned} \tag{1}$$

It is notable that even at the future upgrades of the LHC, these bounds would not be improved considerably. For example, the future upper bounds on $Br(t \to qZ)$ have been predicted to be 0.01% at 95% CL at 14 TeV center-of-mass energy with 3000 fb^{-1} of integrated luminosity of data [28,29]. The branching fraction of $Br(t \to q\gamma)$ would be reachable down to 10^{-4} for $q = c$ and 10^{-5} for $q = u$ at the integrated luminosity of 3000 fb^{-1} at the LHC [30]. Therefore, an important task is to look at the future colliders potential to search for the anomalous FCNC couplings, in particular the e^-e^+ colliders such as International Linear Collider (ILC) [31–38], Compact Linear Collider (CLIC) [39–42], Circular Electron–Positron Collider (CEPC) [43,44] and the Future Circular

E-mail addresses: Hamzeh.Khanpour@mail.ipm.ir (H. Khanpour), Sara.Khatibi@cern.ch (S. Khatibi), Khatiri@ipm.ir (M.K. Yanehsari), Mojtaba@cern.ch (M.M. Najafabadi).

https://doi.org/10.1016/j.physletb.2017.10.047

Collider (FCC-ee) [45–54] which all plan to collect large amount of data and provide high precision measurements.

In Refs. [55,56], an analysis has been performed to probe the sensitivity of a future e^-e^+ collider to top quark FCNC to the photon and a Z boson in the $e^-e^+ \to Z/\gamma \to t\bar{q}$ ($\bar{t}q$) channel. This analysis has been done at the center-of-mass energies of 500 GeV and 800 GeV with the integrated luminosity of up to 1 ab^{-1} without including the effects of parton showering, hadronization, and decay of unstable particles. However, the analysis considers cases with and without the beam polarization to estimate the sensitivity to $tq\gamma$ and tqZ FCNC couplings.

The future large scale circular Electron–Positron collider (FCC-ee) would be one of the high-precision and high-luminosity machines which will be able to perform precise measurements on the Higgs boson, top-quark, Z and W bosons [45,57]. Due to the expected large amount of data and large production rates, FCC-ee can provide an excellent opportunity for precise studies, in particular in the top quark sector. FCC-ee is designed to be working at the center-of-mass energy up to the $t\bar{t}$ threshold mass, i.e. $\sqrt{s} = 350$ GeV. The goal is to reach to a luminosity of $L = 1.3 \times 10^{34}$ $cm^{-2}\,s^{-1}$ [45,57].

In this paper, our aim is to study the anomalous FCNC top couplings, $tq\gamma$ and tqZ, via single top quark production in the FCC-ee at two different center-of-mass energies of 240 GeV and 350 GeV. The final state consists of a top quark in association with a light-quark. We consider the leptonic decay of the W boson in top quark decay, ($t \to Wb \to \ell\nu_\ell b$, where $\ell = e, \mu$). In the analysis, we take into account parton shower, hadronization and decays of unstable particles as well as the detector effects. We present upper limits on the branching ratios at 95% C.L in terms of the integrated luminosity. Finally, the results are compared with the present and future results from the LHC experiments.

The paper is organized as follows. In Section 2, we present the theoretical framework which describes the top quark FCNC couplings to a photon and a Z boson. The Monte Carlo event generation, detector simulation and signal separation from backgrounds are described in Section 3. In Section 4, the results of the sensitivity estimation are presented. Finally, Section 5 includes our summary and conclusions.

2. Theoretical formalism

The anomalous FCNC couplings of a top quark with a photon and a Z boson can be written in a model independent way using an effective Lagrangian approach. The lowest order terms describing $tq\gamma$ and tqZ couplings have the following form [4,21,23,56,58–62]:

$$\begin{aligned}\mathcal{L}_{\rm eff} = \sum_{q=u,c} \Bigg[& e\lambda_{tq}\bar{t}(\lambda^v - \lambda^a\gamma^5)\frac{i\sigma_{\mu\nu}q^\nu}{m_t}qA^\mu \\ & + \frac{g_W}{2c_W}\kappa_{tq}\bar{t}(\kappa^v - \kappa^a\gamma^5)\frac{i\sigma_{\mu\nu}q^\nu}{m_t}q\,Z^\mu \\ & + \frac{g_W}{2c_W}X_{tq}\,\bar{t}\gamma_\mu(x^L P_L + x^R P_R)q\,Z^\mu \Bigg] + \text{h.c.}\,,\end{aligned} \tag{2}$$

where λ_{tq}, κ_{tq} and X_{tq} are dimensionless real parameters that denote the strength of the anomalous FCNC couplings. In the above effective Lagrangian, the chirality parameters are normalized to $|\lambda^a|^2 + |\lambda^v|^2 = |x^L|^2 + |x^R|^2 = |\kappa^v|^2 + |\kappa^a|^2 = 1$ and $P_{L,R}$ are the left- and right-handed projection operators, $P_{L,R} = \frac{1}{2}(1 \mp \gamma^5)$. The anomalous FCNC interactions $tq\gamma$ and tqZ lead to production of a top quark in association with a light quark in Electron–Positron collisions. The Feynman diagram for this process is shown in Fig. 1 including the subsequent leptonic decay of the W boson in the top quark decay. In Table 1, the cross sections of $e^- + e^+ \to t\bar{u} + t\bar{c} + \bar{t}u + \bar{t}c$ including the branching ratio of the top quark decays into a W boson and a b-quark, and W boson decays into a charged lepton (muon and electron) and a neutrino are presented. The cross sections are shown at two different center-of-mass energies of 240 and 350 GeV. It should be pointed out that the cross sections due to photon and Z boson exchange are different and depend on the type of FCNC coupling. The contribution of photon and Z boson exchange with the $\sigma^{\mu\nu}$ coupling increases with the energy of the center-of-mass. This is because of the presence of an additional momentum factor q^ν in the effective Lagrangian.

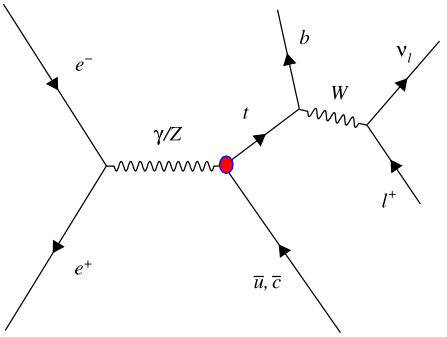

Fig. 1. The Feynman diagram for production of a top in association with a light quark due to the anomalous couplings $tq\gamma$ and tqZ in Electron–Positron collisions.

Table 1
Cross-sections (in fb) of $\sigma(e^- + e^+ \to t\bar{u} + t\bar{c} + \bar{t}u + \bar{t}c) \times Br(t \to Wb \to l\nu b)$ with $\ell = e, \mu$ for three signal scenarios, $tq\gamma$, tqZ (vector–tensor) before applying any cut.

$\sqrt{s}$	240 GeV	350 GeV
FCNC coupling	σ (fb)	σ (fb)
$tq\gamma$	$2154(\lambda_{tq})^2$	$3832(\lambda_{tq})^2$
tqZ ($\sigma_{\mu\nu}$)	$1434(\kappa_{tq})^2$	$2160(\kappa_{tq})^2$
tqZ (γ_μ)	$916(X_{tq})^2$	$786(X_{tq})^2$

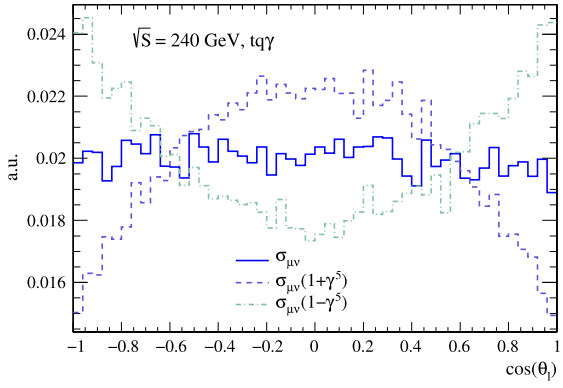

Fig. 2. The distribution of the cosine of the angle between the outgoing charged lepton with the z-axis for $tq\gamma$ with different chirality assumptions at the center-of-mass energy of 240 GeV.

According to the three independent terms of the Lagrangian, there are three possible scenarios to produce single top quark plus a light quark. In this analysis, all three terms of the Lagrangian are investigated independently with the following sets of the chirality parameters: $\lambda^v = 1, \lambda^a = 0$ for $tq\gamma$, for vector like coupling of tqZ: $x^L = x^R$ while for tensor FCNC coupling of tqZ: $\kappa^v = 1, \kappa^a = 0$. In case of observing an excess indicating FCNC signal, the angular distribution of the outgoing particles can be used to determine the chirality of the FCNC couplings. In Fig. 2, the distributions of the

Table 2
Cross-sections (in fb) for the three signal scenarios, $tq\gamma$, tqZ (vector and tensor) and the corresponding $W^{\pm}jj$ and $Z\ell^{\pm}\ell^{\pm}$ SM backgrounds passing sequential cuts at $\sqrt{s}$ = 240 GeV.

$\sqrt{s} = 240$ GeV	Signal			Background	
Cuts	$tq\gamma$	tqZ $(\sigma_{\mu\nu})$	tqZ (γ_{μ})	$W^{\pm}jj$	$Z\ell^{\pm}\ell^{\pm}$
Cross-sections (in fb)	$2154.0(\lambda_{tq})^2$	$1434.0(\kappa_{tq})^2$	$916.0(X_{tq})^2$	4881.2	3588.4
$1\ell + \lvert\eta^{\ell}\rvert < 2.5 + P_T^{\ell} > 10 + \lvert\vec{p}_{\rm miss}\rvert > 10$	$1679.8(\lambda_{tq})^2$	$1117.8(\kappa_{tq})^2$	$715.6(X_{tq})^2$	3886.3	100.1
$2jets + \lvert\eta^{jets}\rvert < 2.5 + P_T^{jets} > 10$	$1393.3(\lambda_{tq})^2$	$927.3(\kappa_{tq})^2$	$590.9(X_{tq})^2$	3459.1	59.7
$n_{b-jet} = 1$	$900.5(\lambda_{tq})^2$	$598.7(\kappa_{tq})^2$	$381.8(X_{tq})^2$	185.3	15.3

Table 3
Cross-sections (in fb) for three signal scenarios, $tq\gamma$, tqZ (vector and tensor) and the corresponding $W^{\pm}jj$, $t\bar{t}$ and $Z\ell^{\pm}\ell^{\pm}$ SM backgrounds passing sequential cuts at $\sqrt{s}$ = 350 GeV.

$\sqrt{s} = 350$ GeV	Signal			Background		
Cuts	$tq\gamma$	tqZ $(\sigma_{\mu\nu})$	tqZ (γ_{μ})	$W^{\pm}jj$	$t\bar{t}$	$Z\ell^{\pm}\ell^{\pm}$
Cross-sections (in fb)	$3832.0(\lambda_{tq})^2$	$2160.0(\kappa_{tq})^2$	$786.0(X_{tq})^2$	3221.1	62.53	4085.0
$1\ell + \lvert\eta^{\ell}\rvert < 2.5 + P_T^{\ell} > 10 + \lvert\vec{p}_{\rm miss}\rvert > 10$	$2984.2(\lambda_{tq})^2$	$1680.2(\kappa_{tq})^2$	$614.6(X_{tq})^2$	2447.6	40.5	129.5
$2jets + \lvert\eta^{jets}\rvert < 2.5 + P_T^{jets} > 10$	$2499.1(\lambda_{tq})^2$	$1405.6(\kappa_{tq})^2$	$507.9(X_{tq})^2$	2175.5	0.65	77.7
$n_{b-jet} = 1$	$1614.1(\lambda_{tq})^2$	$909.0(\kappa_{tq})^2$	$328.4(X_{tq})^2$	112.4	0.43	20.3

cosine of the angle between the outgoing charged lepton with respect to the z-axis (beam axis) are depicted for the $tq\gamma$ signal scenario with three independent types of couplings: $(\lambda^v = 1, \lambda^a = 0)$, $(\lambda^v = \frac{1}{\sqrt{2}}, \lambda^a = \frac{1}{\sqrt{2}})$ and $(\lambda^v = \frac{1}{\sqrt{2}}, \lambda^a = -\frac{1}{\sqrt{2}})$ at $\sqrt{s} = 240$ GeV. As it can be seen, for the type of coupling with no γ^5 the angular distribution is quite flat while for the type of coupling with projection operator $1 \pm \gamma^5$, the distribution has a behavior like a parabola with opposite shapes depending on the sign of the axial term.

The branching ratios for the top quark FCNC decays of $t \to qZ$ and $t \to q\gamma$ are obtained as the ratio of $\Gamma(t \to qZ)$ or $\Gamma(t \to q\gamma)$ to the width of $t \to b + W$ which take the following forms in the FCNC weak coupling approximation:

$$Br(t \to qZ)(\gamma_{\mu}) = 0.47 \times |X_{tqZ}|^2,$$
$$Br(t \to qZ)(\sigma_{\mu\nu}) = 0.37 \times |\kappa_{tqZ}|^2,$$
$$Br(t \to q\gamma) = 0.43 \times |\lambda_{tq\gamma}|^2.$$

3. Analysis strategy

As we have mentioned before, this study is dedicated to probe the $tq\gamma$ and tqZ FCNC couplings via single top quark production at FCC-ee. The results will be presented at different center-of-mass energies of the colliding Electron–Positron. In this section, the details of the event generation and Monte Carlo simulation for signal and backgrounds, event selection, and multivariate analysis to separate signal process from SM background processes will be presented.

3.1. Event generation and simulation

The signal process is defined as $e^-e^+ \to Z/\gamma \to t\bar{q}$ $(\bar{t}q)$, where q is an up or a charm quark. The top quark decays through SM, $t \to W^+b \to \ell^+\nu_{\ell}b$ and $\bar{t} \to W^-\bar{b} \to \ell^-\overline{\nu}_{\ell}\bar{b}$. Therefore, the final state consists of a charged lepton, missing energy, a b-jet and a light jet.

In order to simulate and generate the signal events, the effective Lagrangian describing the FCNC couplings is implemented with the FeynRules package [63–67], then the model has been imported to a UFO module [68] and inserted in MadGraph 5 package [69,70].

Based on the expected signature of the signal process, the main background contribution is originating from $W^{\pm}jj$ production when the W boson decays leptonically, i.e. $e^+e^- \to W^{\pm}jj \to \ell^+\nu_{\ell}jj(\ell^-\overline{\nu}_{\ell}jj)$. Other backgrounds to the signal include the $t\bar{t}$ events in semi-leptonic channel and $Z\ell^{\pm}\ell^{\pm}$ (with hadronic decay of the Z boson). All of these backgrounds are generated at leading order with MadGraph 5. The cross sections of the background processes at the center-of-mass energies of $\sqrt{s}$ = 240 and 350 GeV are presented in the first row of Tables 2 and 3.

We employ Pythia 8.1 package [71–74] for parton showering, hadronization and decay of unstable particles. To reconstruct jets the FastJet package [75–77] with an anti-k_t algorithm [78,79] with a cone size of 0.5 is used. Then the delphes 3 package [80,81] is employed to model the detector performance. We present the results with 70% for the efficiency of b-tagging, a mistagging rate of 10% for charm-quark jets and 1% for other light-flavor jets. It will be shown that the b-tagging requirement plays an important role to reject the background contributions, in particular, $W^{\pm}jj$ and $Z\ell^{\pm}\ell^{\pm}$. The jet energies are smeared in delphes according to the following relation [82]:

$$\frac{\Delta E_{jets}}{E_{jets}} = \frac{30\%}{\sqrt{E_{jets}\ (\rm GeV)}}. \tag{3}$$

The detector performance modeling of leptons (electrons and muons) is taken similar to a CMS-like detector which has been described in Ref. [83].

Events are preselected by requiring only one charged lepton (electron or muon) with $p_T^{\ell} \geq 10$ GeV and $|\eta^{\ell}| < 2.5$. No specific requirement is applied as for trigger condition however the presence of an energetic charged lepton is assumed to be enough. We require to have exactly two jets in each event with $p_T^{jet} \geq 10$ GeV and $|\eta^{jet}| < 2.5$, from which only one is required to be tagged as a b-quark jet.

The events are rejected in which the charged leptons are not isolated. These requirements are useful to suppress the contribution of background events in particular from the top quark pair production.

The four-momentum of the neutrino is determined without any ambiguity from the missing momentum of the event. The missing momentum is required be greater than 10 GeV. To reconstruct the signal topology, first the W boson momentum is reconstructed from the momenta of the charged lepton and the neutrino as $p_W = p_l + p_{\nu}$. The top quark four-momentum is obtained by combining the reconstructed W boson with the b-tagged jet. The mass distribution of the reconstructed top quark is illustrated in Fig. 3

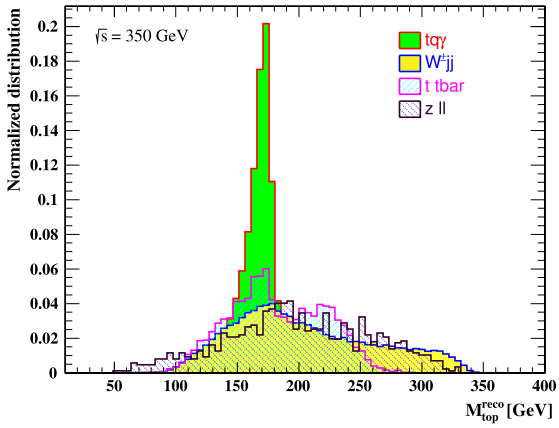

Fig. 3. The normalized reconstructed top quark mass distributions for signal ($tq\gamma$) and the corresponding $W^{\pm}jj$, $t\bar{t}$ and $Z\ell^{\pm}\ell^{\pm}$ SM background processes at $\sqrt{s} =$ 350 GeV. The signal has been shown with $\lambda_{tq} = 0.1$.

for $tq\gamma$ signal and for background processes $W^{\pm}jj$, $t\bar{t}$ and $Z\ell^{\pm}\ell^{\pm}$. Another source of background process is the single top quark production $e^-e^+ \to t + \bar{b} + W^-$ (and $e^-e^+ \to \bar{t} + b + W^+$) which has been found to be extremely negligible due to the requirement on the number of jets ($n_{jets} = 2$) and also vetoing additional charged lepton.

The distribution is at the center-of-mass energy of 350 GeV. As expected the reconstructed top quark mass distribution for signal has a peak around the top quark mass while the background processes have an almost flat distribution with no sharp peak. The top quark pair background process also has an almost sharp peak on the top quark mass due to the fact that the charged lepton, neutrino, and b-jet are coming from one of the top quarks. The $W^{\pm}jj$ background has a broad invariant mass distribution because the b-jet candidate is not originating from the decay of a top quark.

3.2. Separation of signal from background

In order to reduce the SM background processes which have different topologies from the signal events, a multivariate technique [84–88] is used. In particular, in this analysis the Boosted Decision Trees (BDT) is exploited to separate the signal process from backgrounds and to optimize the signal significance. After the preselection cuts described in the previous section which consists of the detector acceptance cuts, and including the effects of b-tagging and mis-tagging, around 40–45% of the signal events and 1–4% of background events survive. The cross sections of signal in all scenarios and the corresponding SM backgrounds at two center-of-mass energies after the preselection cuts are presented in Tables 2 and 3 for $\sqrt{s}$ = 240 and 350 GeV, respectively.

These preselection cuts are generally loose on a single variable and remove a large fraction of the background events while barely reducing also the signal events. As it was mentioned, in this analysis a BDT is trained to obtain a better separation of signal from background events. All the background processes are considered in the training based on their corresponding weights. The choice of proper set of variables is important to achieve a good separation of signal from SM background events and to avoid overtraining. We select those variables which have the best possible discrimination power between signal and background processes. The following variables are used in the analysis:

- $\Delta R(\ell, b-jet)$: the angular separation between the lepton and b-jet
- p_T^{b-jet} and η^{b-jet}: the transverse momentum and pseudorapidity of the b-jet
- M_{top}^{rec}: the reconstructed top quark mass
- E^{ℓ} and η^{ℓ}: the energy and pseudorapidity of the charged lepton
- P_T^{top}: the transverse momentum of reconstructed top-quark
- $E^{light-jet}$: the energy of the light jet

The distributions of some of these variables are shown in Fig. 4. These distributions are corresponding to the signal scenario with anomalous $tq\gamma$ coupling at the center-of-mass energy of 350 GeV. For all signal scenarios $tq\gamma$, $tqZ(\gamma^{\mu})$ and $tqZ(\sigma_{\mu\nu})$ the same variables are used as the inputs of the BDT. As an example, the distribution of the BDT output for the $tq\gamma$ signal and the contributing backgrounds is presented in Fig. 5 for the center-of-mass energy of 350 GeV. In spite of the overwhelming background contributions and the expected small number of signal events, the BDT performs quite well. The BDT response has been checked in terms of discrimination power from the receiver operator characteristic (ROC) of the BDT output. The criteria to apply the optimum cut on the BDT output is based on the best achievable signal significance. For the $tq\gamma$ study at the center-of-mass energy of 350 GeV, the highest signal significance is obtained at the BDT cut value of 0.0055. The BDT cut values are different for various signal scenarios and center-of-mass energies. We perform the analyses separately at the center-of-mass energies of 240 and 350 GeV.

The cross sections of the signal and the $W^{\pm}jj$, $t\bar{t}$ and $Z\ell^{\pm}\ell^{\pm}$ background processes after performing the multivariate analysis are presented in Table 4. As can be seen from this table, the background rejection rate varies at different center-of-mass energies. For all signal scenarios, the background rejection rates after the multivariate analysis technique are $\sim 10^{-1}$, $\sim 10^{-2}$ at the center-of-mass energies of 240 GeV and 350 GeV, respectively. The discriminating power of the input variables are increasing with the center-of-mass energies of the collision. Going to higher energies the overlapping between the signal and background distributions is reduced. In particular, this happens for the top mass, lepton energy and the top quark transverse momentum distributions. Larger background suppression is achieved for the tqZ signal with $\sigma_{\mu\nu}$ coupling with respect to the γ_{μ} coupling. Since the signal-to-background ratio for all signal scenarios increases with the increment of the center-of-mass energy, more sensitivity is expected at larger energies.

4. Sensitivity estimation

To estimate the sensitivities, the upper limits on the branching ratios at 95% C.L is presented. In order to set 95% CL upper limits on the anomalous FCNC couplings and consequently on the branching ratios, the CLs technique is used [89,90]. In the method, the log-likelihoods L_{bkg} and $L_{signal+bkg}$ are defined for the respective background-only and signal + background hypotheses as the multiplication of Poissonian likelihood functions. The p-values for background-only and signal+background hypotheses, i.e. $P_{bkg}(q < q_0)$ and $P_{signal+bkg}(q > q_0)$, are determined using the log-likelihood ratio $q = -2\ln(L_{signal+bkg}/L_{bkg})$ where q_0 is the expected value of statistics q. Limits on the signal cross section is set based on $CL_s = P_{signal+bkg}(q > q_0)/(1 - P_{bkg}(q < q_0))$ which is required to be smaller than 0.05 corresponding to 95% confidence level. More details of the technique could be found in Refs. [89,90].

For the limits calculations the RooStats [91] package is used. The 95% C.L upper limits on the branching ratios of $t \to q\gamma$ and $t \to qZ$ at the center-of-mass energies of 240 GeV and 350 GeV are shown in Table 5 based on an integrated luminosity of 300 fb^{-1}, 3 ab^{-1} and 10 ab^{-1}. As we expected, at each center-of-mass energy, the loosest limits belong to the FCNC transition of $t \to qZ$

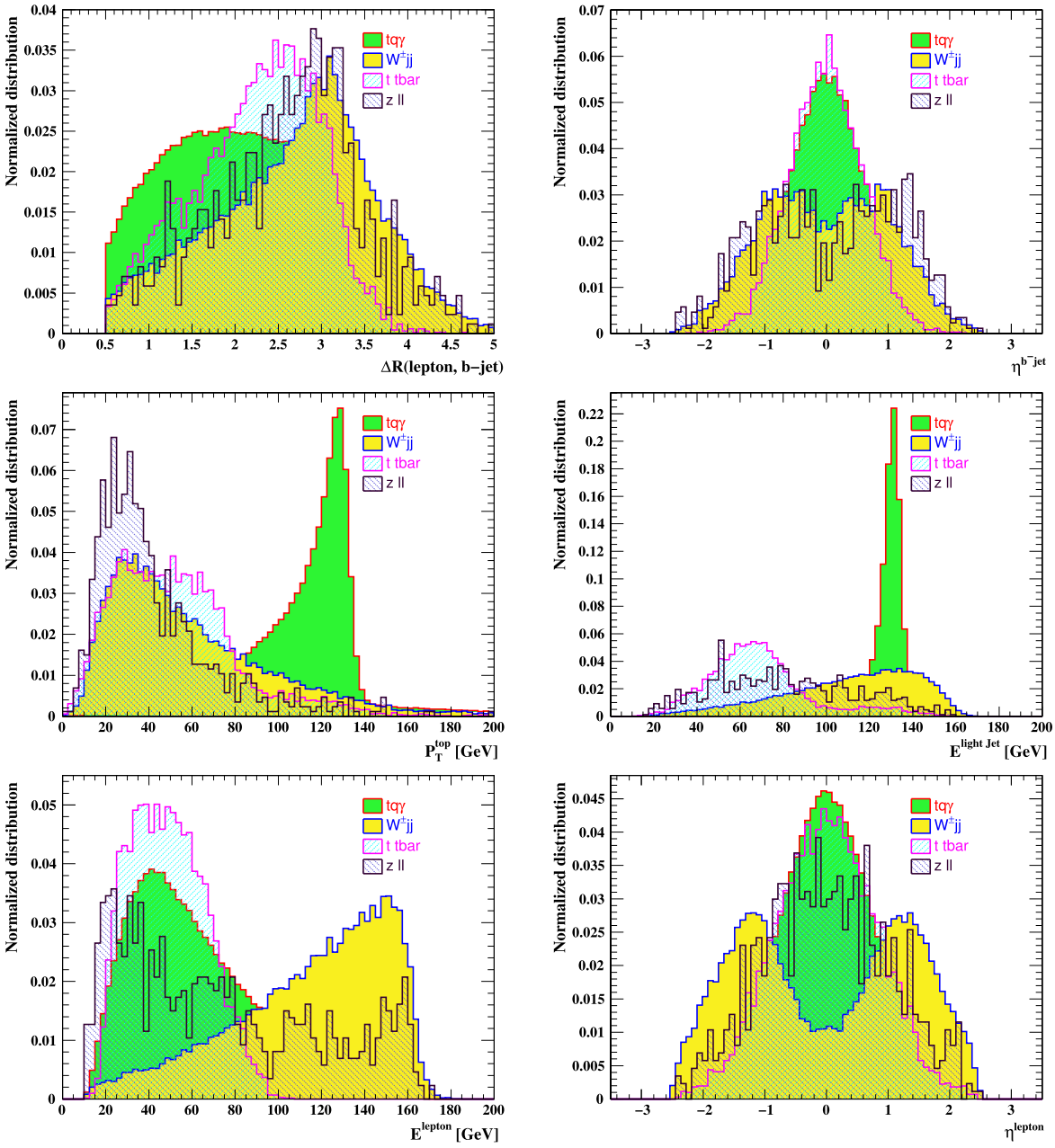

Fig. 4. The normalized distributions of some of the input variables to BDT for the center-of-mass energy of 350 GeV.

with γ_μ-type coupling (10^{-4}). We note that going up from the center-of-mass energy of 240 GeV to 350 GeV, leads to an improvement by a factor of around 3–4 for the integrated luminosity of 300 fb^{-1}.

In order to investigate the sensitivity to b-tagging efficiency and mis-tagging rates, we also present the 95% C.L upper limits on the branching ratios of $t \to q\gamma$ and $t \to qZ$ for 85% of b-tagging efficiency and a 5% mistagging rate for charm quark jets and 1% mistagging rate for the light flavor jets. The results correspond to the center-of-mass energy of 350 GeV for the integrated luminosity of 300 fb^{-1}. As can be seen from Table 6, the higher b-tagging efficiency and smaller mistagging rates could improve the branching ratios by a factor of around 1.6. Charm-tagging algorithm could help to discriminate between tuV and tcV FCNC interactions. It is found that a charm tagging with an efficiency of 30% provides the possibility to separate tuV and tcV and branching fractions of

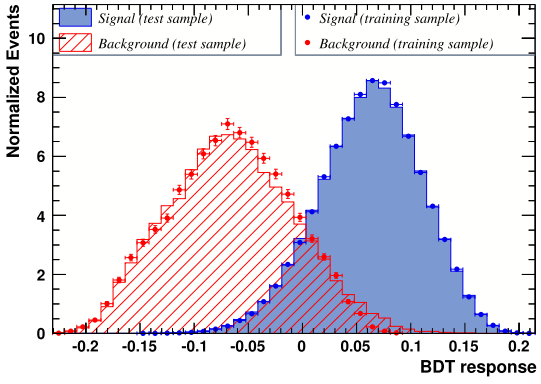

Fig. 5. The distribution of the BDT output for $tq\gamma$ signal and for the background at the center-of-mass energy of 350 GeV.

Table 4
Cross-sections (in fb) of signal and $W^{\pm}jj$, $t\bar{t}$ and $Z\ell^{\pm}\ell^{\pm}$ background processes after performing the multivariate analysis for three signal scenarios, $tq\gamma$, tqZ (vector and tensor) at $\sqrt{s} = 240$ and 350 GeV.

$\sqrt{s} = 240$ GeV	Couplings	Signal	$W^{\pm}jj$ (fb)		$Z\ell^{\pm}\ell^{\pm}$ (fb)
TMVA	$tq\gamma$	$826.32(\lambda_{tq})^2$	26.59	–	5.27
	tqZ $(\sigma_{\mu\nu})$	$547.90(\kappa_{tq})^2$	25.65	–	2.15
	tqZ (γ_{μ})	$354.13(X_{tq})^2$	30.56	–	2.57
$\sqrt{s} = 350$ GeV		Signal	$W^{\pm}jj$ (fb)	$t\bar{t}$ (fb)	$Z\ell^{\pm}\ell^{\pm}$ (fb)
TMVA	$tq\gamma$	$1521.31(\lambda_{tq})^2$	7.59	0.034	1.45
	tqZ $(\sigma_{\mu\nu})$	$856.72(\kappa_{tq})^2$	7.61	0.031	1.45
	tqZ (γ_{μ})	$306.48(X_{tq})^2$	8.49	0.37	1.74

Table 5
The upper limits on the top FCNC decays at 95% C.L obtained at the center-of-mass energies of 240 and 350 GeV for the integrated luminosities of 300 fb^{-1}, 3 ab^{-1} and 10 ab^{-1}.

Integrated luminosity	Branching ratio	240 GeV	350 GeV
300 fb^{-1}	$Br(t \to q\gamma)$	1.23×10^{-4}	3.43×10^{-5}
	$Br(t \to qZ)$ $(\sigma_{\mu\nu})$	1.50×10^{-4}	4.97×10^{-5}
	$Br(t \to qZ)$ (γ_{μ})	3.06×10^{-4}	1.83×10^{-4}
3 ab^{-1}	$Br(t \to q\gamma)$	3.70×10^{-5}	9.86×10^{-6}
	$Br(t \to qZ)$ $(\sigma_{\mu\nu})$	4.50×10^{-5}	1.41×10^{-5}
	$Br(t \to qZ)$ (γ_{μ})	9.25×10^{-5}	5.27×10^{-5}
10 ab^{-1}	$Br(t \to q\gamma)$	2.01×10^{-5}	
	$Br(t \to qZ)$ $(\sigma_{\mu\nu})$	2.44×10^{-5}	
	$Br(t \to qZ)$ (γ_{μ})	5.02×10^{-5}	

Table 6
The upper limits on the top FCNC decays at 95% C.L obtained using the CLs method at the $\sqrt{s}$ = 350 GeV for 85% of b-tagging efficiency and a 5% mistagging rate for charm quark jets and 1% mistagging rate for light flavor jets based on an integrated luminosity of 300 fb^{-1}.

$\sqrt{s}$	$Br(t \to q\gamma)$	$Br(t \to qZ)$ $(\sigma_{\mu\nu})$	$Br(t \to qZ)$ (γ_{μ})
350 GeV	2.19×10^{-5}	3.12×10^{-5}	1.22×10^{-4}

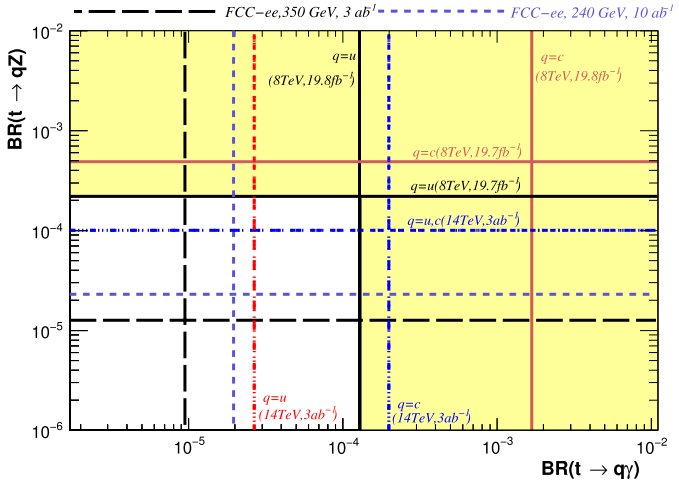

Fig. 6. The current observed upper limits on the $Br(t \to qZ)$ versus $Br(t \to q\gamma)$ at 95% C.L from the recent analyses of the CMS experiment [13,27]. The expected sensitivity from the CMS experiment with 3000 fb^{-1} is also shown [30]. The sensitivity of the FCC-ee with 3 ab^{-1} at the center-of-mass energy of 350 GeV, and with 10 ab^{-1} at the center-of-mass energy of 240 GeV are presented as well. For the FCC-ee case, at a time one coupling is considered.

$t \to c\gamma$ down to 10^5 with an integrated luminosity of 10 ab^{-1} at the center-of-mass energy of 240 GeV.

In Fig. 6, we present the current observed upper limits on the $Br(t \to qZ)$ versus $Br(t \to q\gamma)$ at 95% CL from CMS experiments [13,27]. The expected sensitivity from the CMS experiment with 3000 fb^{-1} in proton–proton collisions at the center-of-mass energy of 14 TeV is also shown [30]. The sensitivity of the FCC-ee with 3 ab^{-1} at the center-of-mass energy of 350 GeV, and with 10 ab^{-1} at the center-of-mass energy of 240 GeV are compared with the CMS experiment results. With an integrated luminosity of 3000 fb^{-1}, CMS is expected to reach to an upper limit of 2.7×10^{-5} on the branching ratio of $t \to u\gamma$, 2.0×10^{-4} on the branching ratio of $t \to c\gamma$, and 1.0×10^{-4} on the branching ratio of $t \to qZ$ ($\sigma_{\mu\nu}$-type coupling). The FCC-ee potential upper limits are expected to be significantly smaller than the expected limits by the future LHC program.

It is worth mentioning that the FCNC transitions can also be probed in $t\bar{t}$ production when a top quark decays anomalously into $q + \gamma$ or $q + Z$. However, it has been found that the limits would be looser than the ones obtained in single top productions [55]. In case of signal observation, LHC would also be able to discriminate between anomalous tuV and tcV ($V = \gamma, Z$) using the charge ratio technique [92]. As we already discussed, this would be possible at the FCC-ee by having an efficient charm tagging technique. Finally, it should be stated that in order to achieve more realistic results, one needs to consider the effects such as the initial state radiation, the luminosity spectrum (LS) and beam bremsstrahlung. However, they are not expected to affect the results significantly [93].

5. Summary and conclusions

Top quark flavor-changing neutral current interactions are extremely forbidden in the SM framework because of the GIM mechanism. The SM predictions for branching ratios of the top quark decay into a photon or a Z boson and an up-type quark are at the order of 10^{-14}. However, several extensions of the SM can enhance the branching ratios by a factor of $10^8 - 10^9$ depending on the model. Therefore, precise measurement of these branching ratios provide an excellent possibility to probe new physics beyond the SM in the top quark sector. While it is impossible to measure the branching ratios with the precisions of order of 10^{-14} to test the SM, observation of sizable branching ratios would indicate new physics beyond the SM. FCC-ee with a clean environment and high luminosity would provide a unique opportunity to measure the properties of top quark and its interactions. In this work, we have investigated the sensitivity and discovery prospects of FCC-ee to the top quark FCNC transitions. We have looked for the FCNC $tq\gamma$ and tqZ couplings in single top-quark production in the process of $e^- + e^+ \to t\bar{q} + \bar{t}q$.

We perform the analysis in a model independent way using the effective Lagrangian approach at the center-of-mass energies of $\sqrt{s}$ = 240 GeV and 350 GeV. In the analysis, we only consider the leptonic (electron and muon) decay of the W boson in the top quark decay. The DELPHES package has been employed to account for the detector modeling. The main background contribution is

coming from $W^{\pm}jj$ production when the W boson decays leptonically, i.e. $e^+e^- \to W^{\pm}jj \to \ell^+\nu_\ell jj(\ell^-\overline{\nu}_\ell jj)$. Other considered backgrounds in this analysis include the top quark pair events in semileptonic decay mode and $Z\ell^{\pm}\ell^{\pm}$ (with hadronic decay of Z). A set of kinematic variables has been proposed as the input variables to a multivariate analysis for discrimination of signal from background processes.

We find the upper limits at 95% CL for three signal scenarios versus the integrated luminosity at the center-of-mass energies of 240 and 350 GeV. The experimental sensitivity increases significantly with the center-of-mass energy. With an integrated luminosity of 300 fb^{-1} at the center-of-mass energy of 350 GeV, upper limits of 3.43×10^{-5} and 4.97×10^{-5} would be obtained on $Br(t \to q\gamma)$ and $Br(t \to qZ)$ ($\sigma_{\mu\nu}$-type), respectively. A looser upper limit of 1.83×10^{-4} on $Br(t \to qZ)$ with γ_μ-type interaction is obtained. It is found that a sensitivity of the order of 10^{-5} at high integrated luminosities would be achievable. We found that FCC-ee would be able to provide us stringent upper limits on the FCNC anomalous couplings and this work could serve as a base for more detailed studies in future in the FCC-ee project.

Acknowledgements

The authors are grateful to Patrizia Azzi and Freya Blekman and other FCC-ee colleagues for many useful discussions and comments. Authors are thankful School of Particles and Accelerators, Institute for Research in Fundamental Sciences (IPM) for financially support of this project. Hamzeh Khanpour also thanks the University of Science and Technology of Mazandaran for financial support provided for this research.

References

[1] S.L. Glashow, J. Iliopoulos, L. Maiani, Phys. Rev. D 2 (1970) 1285.
[2] K. Agashe, et al., Top Quark Working Group, arXiv:1311.2028 [hep-ph].
[3] S. Bejar, J. Guasch, D. Lopez-Val, J. Sola, Phys. Lett. B 668 (2008) 364.
[4] J. Cao, Z. Heng, L. Wu, J.M. Yang, Phys. Rev. D 79 (2009) 054003.
[5] R. Guedes, R. Santos, M. Won, Phys. Rev. D 88 (11) (2013) 114011.
[6] G.A. Gonzalez-Sprinberg, R. Martinez, arXiv:hep-ph/0605335.
[7] R. Coimbra, A. Onofre, R. Santos, M. Won, Eur. Phys. J. C 72 (2012) 2222.
[8] R.A. Diaz, R. Martinez, J. Alexis Rodriguez, arXiv:hep-ph/0103307.
[9] G.r. Lu, F.r. Yin, X.l. Wang, L.d. Wan, Phys. Rev. D 68 (2003) 015002.
[10] G. Couture, M. Frank, H. Konig, Phys. Rev. D 56 (1997) 4213.
[11] G. Aad, et al., ATLAS Collaboration, Eur. Phys. J. C 76 (1) (2016) 12.
[12] G. Aad, et al., ATLAS Collaboration, Eur. Phys. J. C 76 (2) (2016) 55.
[13] V. Khachatryan, et al., CMS Collaboration, J. High Energy Phys. 1604 (2016) 035.
[14] Y.C. Guo, C.X. Yue, S. Yang, Eur. Phys. J. C 76 (11) (2016) 596.
[15] ATLAS Collaboration, ATLAS-CONF-2013-063.
[16] G. Aad, et al., ATLAS Collaboration, J. High Energy Phys. 1406 (2014) 008.
[17] S. Chatrchyan, et al., CMS Collaboration, Phys. Lett. B 718 (2013) 1252.
[18] G. Aad, et al., ATLAS Collaboration, J. High Energy Phys. 1209 (2012) 139.
[19] S. Chatrchyan, et al., CMS Collaboration, Phys. Rev. Lett. 112 (17) (2014) 171802.
[20] Y. Chao, CMS Collaboration, PoS EPS HEP2013 (2013) 069.
[21] V.M. Abazov, et al., D0 Collaboration, Phys. Lett. B 701 (2011) 313.
[22] H. Abramowicz, et al., ZEUS Collaboration, Phys. Lett. B 708 (2012) 27.
[23] V.F. Obraztsov, S.R. Slabospitsky, O.P. Yushchenko, Phys. Lett. B 426 (1998) 393.
[24] P. Achard, et al., L3 Collaboration, Phys. Lett. B 549 (2002) 290.
[25] J. Abdallah, et al., DELPHI Collaboration, Phys. Lett. B 590 (2004) 21.
[26] CMS Collaboration, association with a photon, CMS-PAS-TOP-14-003.
[27] CMS Collaboration, CMS-PAS-TOP-12-039.
[28] CMS Collaboration, CMS-PAS-FTR-13-016.
[29] ATLAS Collaboration, ATL-PHYS-PUB-2012-001, ATL-COM-PHYS-2012-1118.
[30] CMS Collaboration, CMS-DP-2016-064.
[31] K. Fujii, et al., arXiv:1506.05992 [hep-ex].
[32] T. Behnke, et al., arXiv:1306.6329 [physics.ins-det].
[33] T. Barklow, J. Brau, K. Fujii, J. Gao, J. List, N. Walker, K. Yokoya, arXiv:1506.07830 [hep-ex].
[34] D.M. Asner, et al., arXiv:1310.0763 [hep-ph].
[35] G. Moortgat-Pick, et al., Eur. Phys. J. C 75 (8) (2015) 371.
[36] D. Asner, A. Hoang, Y. Kiyo, R. Pöschl, Y. Sumino, M. Vos, arXiv:1307.8265 [hep-ex].
[37] J.E. Brau, R.M. Godbole, F.R.L. Diberder, M.A. Thomson, H. Weerts, G. Weiglein, J.D. Wells, H. Yamamoto, arXiv:1210.0202 [hep-ex].
[38] M. Martinez, R. Miquel, Eur. Phys. J. C 27 (2003) 49.
[39] L. Linssen, A. Miyamoto, M. Stanitzki, H. Weerts, https://doi.org/10.5170/CERN-2012-003, arXiv:1202.5940 [physics.ins-det].
[40] M. Aicheler, et al., https://doi.org/10.5170/CERN-2012-007.
[41] H. Abramowicz, et al., CLIC Detector and Physics Study Collaboration, arXiv:1307.5288 [hep-ex].
[42] P. Lebrun, et al., https://doi.org/10.5170/CERN-2012-005, arXiv:1209.2543 [physics.ins-det].
[43] CEPC-SPPC Study Group, IHEP-CEPC-DR-2015-01, IHEP-TH-2015-01, IHEP-EP-2015-01.
[44] CEPC-SPPC Study Group, IHEP-CEPC-DR-2015-01, IHEP-AC-2015-01.
[45] M. Bicer, et al., TLEP Design Study Working Group, J. High Energy Phys. 1401 (2014) 164.
[46] M. Koratzinos, PoS EPS HEP2015 (2015) 518, arXiv:1511.01021 [physics.acc-ph].
[47] J. Ellis, T. You, J. High Energy Phys. 1603 (2016) 089.
[48] M. Benedikt, K. Oide, F. Zimmermann, A. Bogomyagkov, E. Levichev, M. Migliorati, U. Wienands, arXiv:1508.03363 [physics.acc-ph].
[49] M. Koratzinos, et al., arXiv:1506.00918 [physics.acc-ph].
[50] F. Zimmermann, et al., CERN-ACC-2014-0262.
[51] P. Janot, J. High Energy Phys. 1504 (2015) 182.
[52] D. d'Enterria, https://doi.org/10.1142/9789813224568_0028, arXiv:1602.05043 [hep-ex].
[53] D. d'Enterria, Frascati Phys. Ser. 61 (2016) 17, arXiv:1601.06640 [hep-ex].
[54] D. d'Enterria, et al., arXiv:1512.05194 [hep-ph].
[55] J.A. Aguilar-Saavedra, T. Riemann, arXiv:hep-ph/0102197.
[56] J.A. Aguilar-Saavedra, Phys. Lett. B 502 (2001) 115.
[57] M. Koratzinos, et al., arXiv:1305.6498 [physics.acc-ph].
[58] E. Malkawi, T.M.P. Tait, Phys. Rev. D 54 (1996) 5758.
[59] Y.P. Gouz, S.R. Slabospitsky, Phys. Lett. B 457 (1999) 177.
[60] M. Hosch, K. Whisnant, B.L. Young, Phys. Rev. D 56 (1997) 5725.
[61] J.A. Aguilar-Saavedra, Nucl. Phys. B 812 (2009) 181.
[62] J.A. Aguilar-Saavedra, Acta Phys. Pol. B 35 (2004) 2695, arXiv:hep-ph/0409342.
[63] A. Alloul, N.D. Christensen, C. Degrande, C. Duhr, B. Fuks, Comput. Phys. Commun. 185 (2014) 2250.
[64] N.D. Christensen, C. Duhr, B. Fuks, J. Reuter, C. Speckner, Eur. Phys. J. C 72 (2012) 1990.
[65] B. Fuks, Int. J. Mod. Phys. A 27 (2012) 1230007.
[66] C. Duhr, B. Fuks, Comput. Phys. Commun. 182 (2011) 2404.
[67] N.D. Christensen, P. de Aquino, C. Degrande, C. Duhr, B. Fuks, M. Herquet, F. Maltoni, S. Schumann, Eur. Phys. J. C 71 (2011) 1541.
[68] C. Degrande, C. Duhr, B. Fuks, D. Grellscheid, O. Mattelaer, T. Reiter, Comput. Phys. Commun. 183 (2012) 1201.
[69] J. Alwall, M. Herquet, F. Maltoni, O. Mattelaer, T. Stelzer, J. High Energy Phys. 1106 (2011) 128.
[70] J. Alwall, et al., J. High Energy Phys. 1407 (2014) 079.
[71] P. Skands, S. Carrazza, J. Rojo, Eur. Phys. J. C 74 (8) (2014) 3024.
[72] K. Kong, https://doi.org/10.1142/9789814390163_0004, arXiv:1208.0035 [hep-ph].
[73] J.P. Guillaud, CERN-CMS-NOTE-2000-070, CMS-NOTE-2000-070.
[74] T. Sjostrand, S. Mrenna, P.Z. Skands, J. High Energy Phys. 0605 (2006) 026.
[75] M. Cacciari, G.P. Salam, G. Soyez, Eur. Phys. J. C 72 (2012) 1896.
[76] M. Cacciari, arXiv:hep-ph/0607071.
[77] M. Cacciari, G.P. Salam, Phys. Lett. B 641 (2006) 57.
[78] S. Catani, Y.L. Dokshitzer, M.H. Seymour, B.R. Webber, Nucl. Phys. B 406 (1993) 187.
[79] S.D. Ellis, D.E. Soper, Phys. Rev. D 48 (1993) 3160.
[80] J. de Favereau, et al., DELPHES 3 Collaboration, J. High Energy Phys. 1402 (2014) 057.
[81] A. Mertens, J. Phys. Conf. Ser. 608 (1) (2015) 012045, https://doi.org/10.1088/1742-6596/608/1/012045.
[82] P. Azzi, et al., arXiv:1703.01626 [hep-ph].
[83] G.L. Bayatian, et al., CMS Collaboration, J. Phys. G 34 (6) (2007) 995.
[84] A. Hocker, et al., PoS ACAT (2007) 040, arXiv:physics/0703039 [PHYSICS].
[85] J. Stelzer, A. Hocker, P. Speckmayer, H. Voss, PoS ACAT 08 (2008) 063.
[86] J. Therhaag, TMVA Core Developer Team, AIP Conf. Proc. 1504 (2009) 1013.
[87] P. Speckmayer, A. Hocker, J. Stelzer, H. Voss, J. Phys. Conf. Ser. 219 (2010) 032057.
[88] J. Therhaag, PoS ICHEP 2010 (2010) 510.
[89] A.L. Read, J. Phys. G 28 (2002) 2693.
[90] B. Mistlberger, F. Dulat, arXiv:1204.3851 [hep-ph].
[91] L. Moneta, et al., PoS ACAT 2010 (2010) 057, arXiv:1009.1003 [physics.data-an].
[92] S. Khatibi, M. Mohammadi Najafabadi, Phys. Rev. D 89 (5) (2014) 054011.
[93] H. Hesari, H. Khanpour, M. Khatiri Yanehsari, M. Mohammadi Najafabadi, Adv. High Energy Phys. 2014 (2014) 476490.